Acoustic Backscatter from Salinity Microstructure

HARVEY E. SEIM

Skidaway Institute of Oceanography, Savannah, Georgia

(Manuscript received 4 April 1997, in final form 14 May 1998)

ABSTRACT

The contribution of salinity changes to sound speed fluctuations is often neglected in estimating the scattering cross section at high frequencies (>10 kHz). To examine when salinity might be important, an expression is formulated for the scattering cross section σ that includes salinity and an estimate of the cospectrum of temperature and salinity. Profiles from the southern New England shelf, the Bosphorus, and Puget Sound are used to estimate levels of σ as a function of depth and acoustic frequency. Salinity can increase σ by more than an order of magnitude, particularly at frequencies greater than 100 kHz, when salinity controls the density field. The cospectrum is expected to be large under the same conditions and can potentially negate strong scattering at lower frequencies. An f^{+1} dependence of σ is expected over two decades in frequency when salinity controls density. Multifrequency acoustic systems may be able to distinguish biology and microstructure based on this spectral dependence.

1. Introduction

Studies of turbulent mixing in inshore waters and the coastal zone often make use of high-frequency backscatter systems to produce images of the water column. These unaliased images of the flow field provide invaluable information about the spatial structures being sampled. Examples of remarkable images can be found in Haury et al. (1983), Farmer and Smith (1980), Farmer and Denton (1985), Armi and Farmer (1988), and Wesson and Gregg (1994), to cite a few. Uncertainty remains, however, about the nature of the scatterers and whether they are zooplankton, suspended particles, or turbulent refractive index fluctuations (Farmer and Smith 1980; Haury et al. 1983; Seim et al. 1995).

It is now popular to use echosounding systems to make biomass estimates, assuming scattering models for various zooplankton (e.g., Holliday et al. 1989; Wiebe and Greene 1994). A variety of plankton scattering models are in use (e.g., Stanton et al. 1994; Macaulay 1994) that assume differing shape and composition of the plankton. While in many instances it may be reasonable to assume that plankton are the dominant scatterers (e.g., when there is an obvious diurnal migration of the scatterers), there have been very few attempts to quantify the relative importance of the possible scatterers.

Several studies have suggested that measurable acoustic backscatter can be generated from turbulent refractive index fluctuations. Thorpe and Brubaker (1983) demonstrated experimentally that measurable backscatter was produced by temperature microstructure by towing a sphere in the thermocline of a lake and imaging its wake. They also measured elevated levels of naturally produced temperature microstructure where enhanced backscatter was observed but were unable to make a quantitative comparison. Goodman (1990) estimates the scattering strength due to turbulent refractive index fluctuations for a number of studies and finds that in many cases the predicted levels are quite large. Seim et al. (1995) compared microstructure measurements and calibrated backscatter values from large turbulent billows in a tidal channel and found reasonable agreement, but only at the level of the billows, and concluded that elsewhere in the water column biological scattering dominated. We are unaware of any studies that have simultaneously measured calibrated acoustic returns, biomass concentrations, and turbulence levels. Lacking such an attempt to close an acoustic backscatter budget, the issue remains unresolved.

Models of backscattering from microstructure assume returns are dominated by scattering at the Bragg wavenumber $k_{br} = 2\kappa$, where κ is the acoustic wavenumber. The scattering cross section is then related to the level of the refractive index fluctuation spectrum at k_{br}. Models of the turbulent temperature gradient spectrum are used to estimate the refractive index spectrum (Goodman 1990). Significant backscatter at vertical incidence can result from reflection at a sound speed gradient but is important only when the acoustic wavelength and

Corresponding author address: Harvey E. Seim, Skidaway Institute of Oceanography, 10 Ocean Science Circle, Savannah, GA 31411.
E-mail: seim@skio.peachnet.edu

vertical scale of the gradient are comparable (Ewart 1980). Because the pycnoclines discussed in this paper are at least 1 m in width and the acoustic wavelengths for frequencies greater than 10 kHz are less than 0.15 m, the amount of backscatter due to reflection is negligible. Between 1 and 10 kHz, reflection from 1-m-scale pycnoclines may be important but is not considered further in this study.

Salinity controls the density in the nearshore environments where many of the internal hydraulic phenomena have been observed. Seim et al. (1995) find that the refractive index fluctuations due to salinity microstructure can be equal to that resulting from temperature microstructure at 200 kHz.

This article makes a more detailed examination of the role that salinity microstructure may play in determining the acoustic scattering budget. A formulation for the scattering cross section as a function of acoustic frequency that includes salinity is developed in section 2. This development includes an estimate of the cospectrum of temperature and salt. Three sites—two from inland straits (the Bosphorus in Turkey, and Admiralty Inlet in Puget Sound) and one from a continental shelf (the southern New England shelf)—are then compared. For each site we form the scattering cross section as a function of acoustic frequency and depth from representative profiles of temperature, salinity, and dissipation rates of turbulent kinetic energy (ϵ) and temperature variance (χ). The magnitude and frequency content of the scattering cross section vary widely among these sites and suggest that scattering from salinity microstructure dwarfs that owing to temperature microstructure in regimes where salinity determines the density field.

2. Theory

The reader is referred to Goodman (1990) for a derivation of the relationship of scattering cross section σ to the refractive index fluctuation spectrum ϕ_η. We here start with the one-dimensional, one-sided spectrum of refractive index fluctuations

$$\phi_\eta = a^2\phi_T + b^2\phi_s + 2ab\phi_{sT}, \tag{1}$$

where ϕ_T and ϕ_s are the one-dimensional spectra of temperature T and salinity s and ϕ_{sT} is their cospectrum. The coefficients a and b are the fractional change in sound speed c with temperature and salinity, respectively, defined as

$$a = \frac{1}{c}\frac{\partial c}{\partial T}\bigg|_{s,T}, \qquad b = \frac{1}{c}\frac{\partial c}{\partial s}\bigg|_{s,T}. \tag{2}$$

The relative importance of temperature and salinity to sound speed variations can be examined by forming the ratio of a and b using the vertical gradients of T and s,

$$R_\eta = \frac{a}{b}\delta, \qquad \delta \equiv \frac{\partial T/\partial z}{\partial s/\partial z}. \tag{3}$$

The magnitude of R_η provides a measure of the potential importance of salinity to the backscattered sound field.

The temperature and salinity spectra and the cospectrum are assumed to be dominated by turbulence at the acoustic frequencies of interest (1–10^4 kHz). We use an inertial–convective model for wavenumbers less than $k_* = (\epsilon/\nu^3)^{1/4}/8$, the peak of the transverse shear spectrum in the Panchev and Kesich model (Seim and Gregg 1994), where ν is molecular viscosity; and a viscous–convective model to represent the scalar variance at higher wavenumbers:

$$\phi = A\chi\epsilon^{-1/3}k^{-5/3} \qquad \text{for } k \le k_*$$

$$\phi = \left(\frac{q}{2}\right)^{1/2}\frac{1}{k^2}\frac{\chi}{k_d D}g(\zeta) \quad \text{for } k > k_*, \tag{4}$$

where

$$g(\zeta) = \zeta\left[e^{-\zeta^2/2} - \zeta\int_\zeta^\infty e^{-x^2/2}\,dx\right]$$

is the ''universal'' spectrum, $k_d = (\epsilon/\nu D^2)^{1/4}$ is the diffusive cutoff wavenumber, $\zeta = (2q)^{1/2}k/k_d$, χ is the dissipation rate of scalar variance, D is the scalar diffusivity (for temperature, from this point on), and k is wavenumber. This model is similar to that originally proposed by Batchelor (1959) and approximately that proposed by Dillon and Caldwell (1980). All wavenumbers are expressed in radians per meter except for plotting purposes where we use cycles per meter. The constants are $A = 0.925$ and $q = 3.7$; the value of q is that suggested by Oakey (1982) and we choose A so that the two spectra are equal at k_* (cf. Dillon and Caldwell 1980).

This model is applicable in regions of energetic turbulence; a practical limit might be $\epsilon > 10^{-8}$ W kg^{-1}. When dissipation rates fall below this, as is often the case in the open ocean, the inertial–convective subrange is quite limited in bandwidth and may not be present at all (Dillon and Caldwell 1980). The choice of the constants A and q is also uncertain: Gargett (1985) finds instances of very different values of q and estimates for the position of k_* vary widely (see Dillon and Caldwell 1980; Seim et al. 1995). The values used are believed to give reasonable estimates of the turbulent spectra for the cases presented in this study, but the model may need to be modified if applied in low-energy environments.

The cospectrum ϕ_{sT} remains unmeasured. Similar to Washburn et al. (1996), we estimate the maximum effect the cospectrum can have using the spectral inequality (Bendat and Piersol 1986),

$$\phi_{sT} \le (\phi_s\phi_T)^{1/2} = A(\chi_s\chi)^{1/2}\epsilon^{-1/3}k^{-5/3} \qquad \text{for } k \le k_*$$

$$= \left(\frac{q}{2}\right)^{1/2}\frac{1}{k^2}\left(\frac{\chi_s\chi}{k_{ds}k_d D_s D}\right)^{1/2}[g(\zeta)g(\zeta_s)]^{1/2} \quad \text{for } k > k_*, \tag{5}$$

where χ_s is the dissipation rate of salt variance, $\zeta_s = (2q)^{1/2}k/k_{ds}$, $k_{ds} = (\epsilon/\nu D_s^2)^{1/4}$, and D_s is the molecular diffusivity of salt.

Last, we relate refractive index fluctuations to the scattering cross section with (Seim et al. 1995)

$$\sigma = -\frac{k_{\rm br}^3}{32}\frac{d}{dk}\phi_\eta(k_{\rm br}), \tag{6}$$

where σ is the scattering cross section per unit volume per unit solid angle. Combining Eqs. (1), (4), (5), and (6) we can estimate σ given profiles of s, T, ϵ, and χ, where χ is now the dissipation rate of temperature variance. We also require an estimate of χ_s, which, because of the small value of the molecular diffusivity of salt, remains unmeasured. Assuming the scalar dissipation rates are proportional to the square of the mean vertical gradients (Gregg 1984), we use $\chi_s = \chi/\delta^2$. The resulting equation is

$$\sigma = A\frac{5}{96}\frac{\chi}{\epsilon^{1/3}}k_{\rm br}^{1/3}\left(a^2 + \frac{b^2}{\delta^2} + \frac{2ab}{\delta}\right) \quad \text{for } k \le k_{\rm int},$$

$$\sigma = q\left(\frac{\nu}{\epsilon}\right)^{1/2}\frac{\chi k_{\rm br}}{32}\left[a^2 e^{-\zeta^2/2} + \frac{b^2}{\delta^2}e^{-\zeta_s^2/2} + \frac{ab}{\delta[g(\zeta)g(\zeta_s)]^{1/2}} \times \left(\left(\frac{D_s}{D}\right)^{1/4} g(\zeta)e^{-\zeta_s^2/2} + \left(\frac{D}{D_s}\right)^{1/4} g(\zeta_s)e^{-\zeta^2/2}\right)\right] \quad \text{for } k > k_{\rm int}, \tag{7}$$

where $k_{\rm int} = (5/3)^{3/2}k_*$. Note that the cospectral terms (those containing ab) include δ, which can be either positive or negative, depending on the local T–s relationship. To compare the contribution that individual terms make to σ we define the following terms: σ^T is temperature only (a^2 terms); σ^{sT} is salinity and temperature (a^2 and b^2 terms); and σ^{sTc} is salinity, temperature, and cospectrum (all terms).

3. Observations

Representative profiles from three sites are compared to examine the importance of salinity in generating acoustic backscatter. The profiles are from the Admiralty Inlet in Puget Sound [spring 1988 (Seim and Gregg 1994), profile 54], the Bosphorus (fall 1994), and from the shelf off southern New England (Coastal Mixing and Optics cruise, fall 1996). The sites represent estuarine and coastal environments and should give some idea of the variability in scattering to be expected between these environments. Profiles are shown in Fig. 1.

The profiles are, for the most part, stably stratified. The profiles have been averaged over 2–3 m so that vertical gradients (i.e., δ) are reasonably well resolved. At the shelf site the density gradient is more uniform with depth than at the estuarine sites where a strong middepth pycnocline exists.

The dissipation rate profiles (Fig. 1) exhibit the broad dynamic range characteristic of these fields. For two of the datasets the estimates are preliminary, and in particular, χ for the Bosphorus may be underestimated because of probe response limitations (Gregg 1999). To assess the quality of χ we compare the measured values with estimates based on

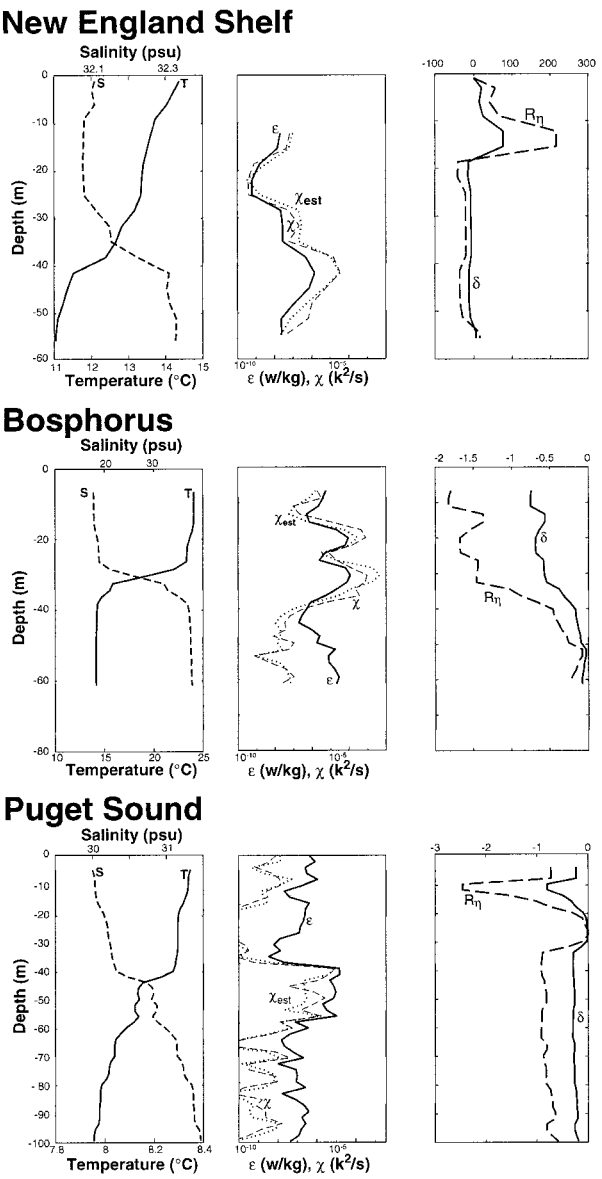

FIG. 1. (left panels) Temperature and salinity; (middle panels) ϵ, χ, and $\chi_{\rm est}$; and (right panels) δ and R_η profiles for (a) shelf off southern New England, (b) the Bosphorus in Turkey, and (c) Admiralty Inlet in Puget Sound.

$$\chi_{\epsilon{\rm st}} = \gamma\epsilon\frac{2\overline{T_z}}{N^2}, \tag{8}$$

where the buoyancy frequency squared $N^2 = -g/\rho(\partial\rho/\partial z)$, ρ is fluid density, g is the acceleration due to gravity, z is the vertical coordinate and is positive upward, and we assume the mixing efficiency $\gamma = 0.2$ (Gregg 1987).

Profiles of χ_{est} and χ differ significantly at the main pycnocline in the Bosphorus, where χ_{est} exceeds χ by as much as a factor of 10 (Fig. 1). At the other sites the measured and estimated values are in good agreement, especially for maximum values. At all locations maxima in χ occur where the mean temperature gradients are large. Values of χ are comparable for the New England shelf and Bosphorus, smaller for Puget Sound, and values of ϵ are largest in the Bosphorus. In the analysis below we use χ_{est} for the Bosphorus data because of the potential problems associated with the probe resolution.

Plots of δ for the sites indicate the relative importance of salinity and temperature to the vertical density gradient (Fig. 1). Temperature determines the density field in the upper portion of the water column on the New England shelf and leads to large values of δ. Below this a consistent *T*–*s* relation gives values of δ from -5 to -10. In the Bosphorus $-1 < \delta < 0$ over the entire water column, reflecting the large vertical changes in salinity often observed in inland waters. For Puget Sound, δ is small over the entire water column, reaching a minimum near 30 m in a thermostad. Also plotted in Fig. 1 are the profiles of R_η. They closely follow the vertical variations of the δ profiles but the values are roughly a factor of 2 larger, reflecting the greater importance of temperature in determining sound speed. Despite this, $-3 < R_\eta < 0$ for the Bosphorus and Puget Sound. Salinity structure is as important as temperature in determining sound speed variations in the estuarine environments.

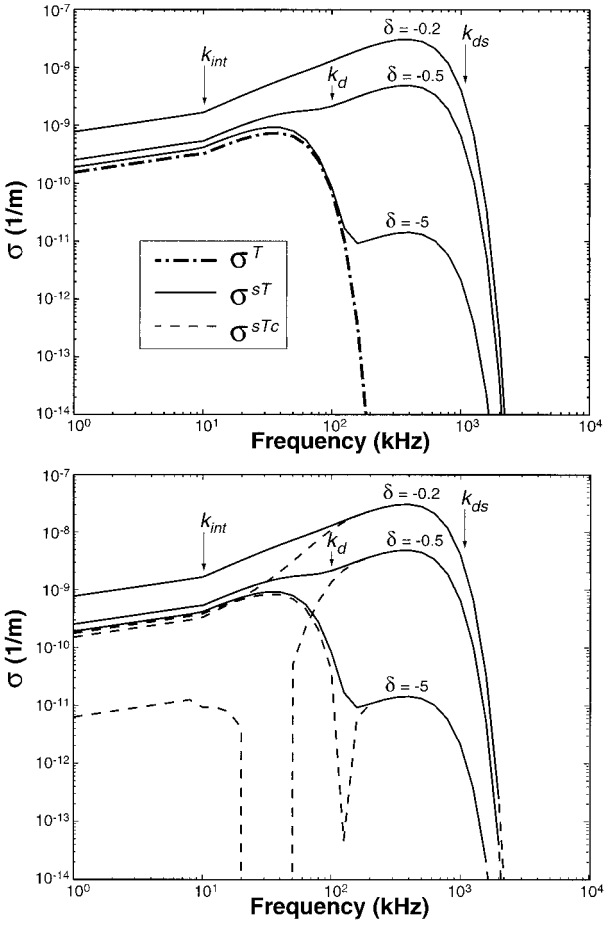

FIG. 2. (top) Temperature-only (σ^T) and salinity and temperature (σ^{sT}) spectra. (bottom) Comparison of salinity, temperature, and cospectra (σ^{sTc}) and σ^{sT} spectra. The influence of the cospectrum is strongly dependent on the value of δ. A range of δ values is shown. For an estuary, $\delta = -0.2$ ($R_\eta = -0.5$), while for the shelf $\delta = -5$ ($R_\eta = -27$); the value of -0.5 is intermediate ($R_\eta = -1.2$) and is most strongly effected by the cospectrum. For all spectra $\epsilon = 10^{-8}$ W kg^{-1} and $\chi = 10^{-6}$ K^2 s^{-3}. Transitions between turbulent subranges are marked by the corresponding wavenumbers.

4. Predicted scattering cross sections

The scattering cross section as a function of acoustic frequency, as given in (7), is plotted in Fig. 2 for three values of δ to demonstrate the potential variability in the spectrum. The σ^T spectrum cuts off near the acoustic frequency corresponding to k_d, the diffusive cutoff wavenumber of temperature (Fig. 2). Including salinity (σ^{sT}) increases the bandwidth of σ by about a factor of 10. For $\delta = -5$ (a value representative of the shelf) the scattering is much weaker at these frequencies, but not necessarily negligible, and leads to a ledge at 100–1000 kHz in the σ spectrum. For $\delta = -0.2$ (representative of an estuary) the salinity contribution dominates σ and shifts the spectral maximum to frequencies 10 times that of the σ^T spectrum. The increase in scattering cross section at high frequencies can be dramatic. The frequency of peak response is strongly affected by the magnitude of ϵ, as will be apparent from the examples below.

The effect of the cospectrum is illustrated in Fig. 2b. For $|\delta| \gg 1$, the cospectrum is small and its principal influence is to introduce a narrow notch near $f(k_d)$, where $f(x) = c_o x/(4\pi)$ is the frequency (in Hz) corresponding to wavenumber x (in rad m^{-1}). For $|\delta| < 1$ the cospectrum is nearly as large as the combined temperature and salinity effects. Below $f(k_{\text{int}})$, the level of the inertial–convective subrange is significantly reduced. When $|R_\eta| < 1$, the impact of the cospectrum gradually decreases above $f(k_{\text{int}})$ and near $f(k_d)$ the cospectrum falls to zero. When $R_\eta \approx -1$ (the $\delta = -0.5$ case), the cospectrum equals the sum of the temperature and salinity spectrum in the viscous–convective subrange and a deep notch develops at these frequencies.

We estimate the maximum effect of the cospectrum, and it is unlikely that a perfect correlation is maintained as the diffusive scales for temperature are approached (Washburn et al. 1996). For large δ the narrow notch is unlikely to be observed because it occurs at scales where diffusion destroys gradients in temperature. For small δ, and, in particular for $R_\eta \approx 1$, there may be a significant drop in σ because the notch occurs at larger scales.

The dependence of the importance of the cospectrum on δ can be explained by examining (7). For $k < k_{\text{int}}$,

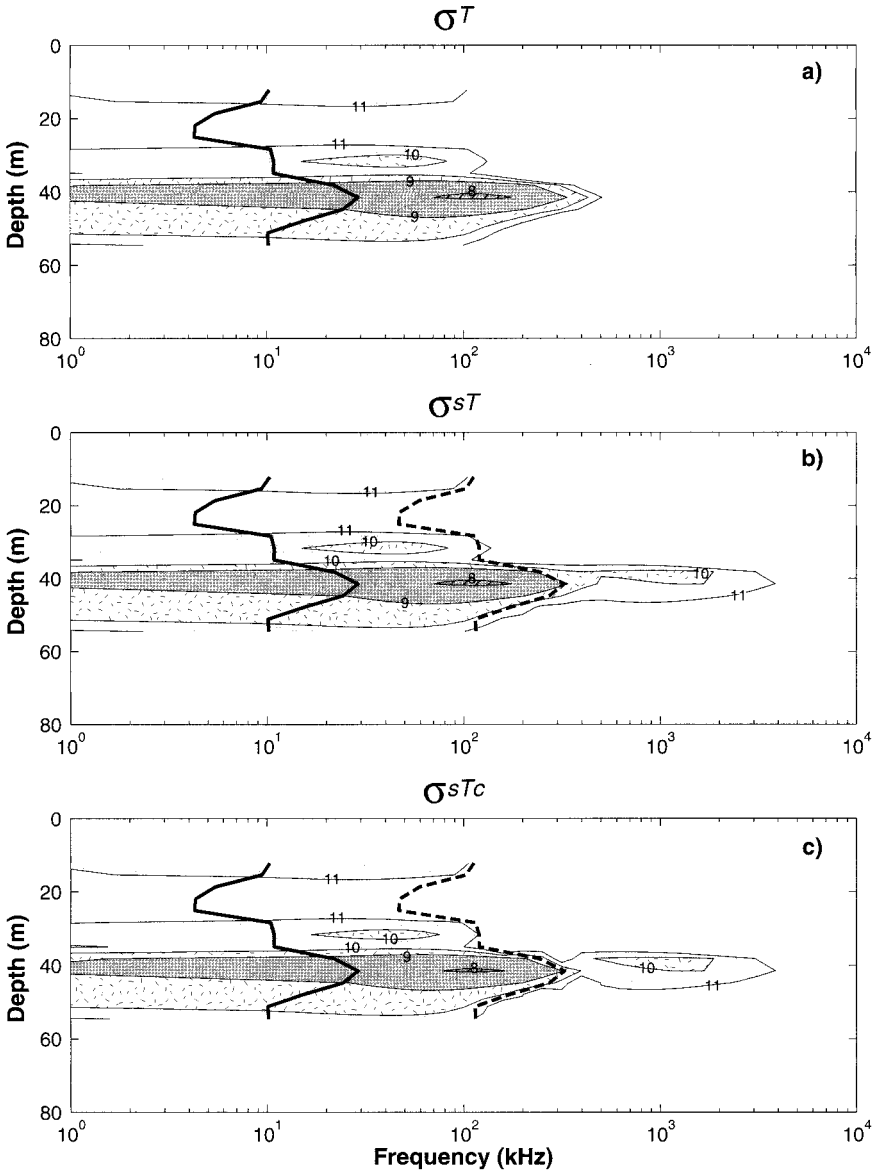

FIG. 3. Contours of σ as a function of depth and acoustic frequency for the New England Shelf: (a) σ^T, (b) σ^{sT}, and (c) σ^{sTc}. Levels above 10^{-11} m^{-1} are contoured every factor of 10. The transition frequencies $f(k_{\text{int}})$ (solid line) and $f(k_d)$ (dashed line) are shown as thick lines. Including salinity introduces a ledge of increased σ over 100–1000 kHz only where δ is a minimum and the dissipation rates are large. The cospectrum has little influence.

for example, the term in parentheses is a quadratic expression $a^2 + 2ab/\delta + b^2/\delta^2$: zeros occur where $a = -b/\delta$. In general $a > b$, and they are of the same sign, so only when $-1 < \delta < 0$ can the cospectrum become large enough to cancel the contributions from the temperature and salinity spectra.

Forming σ as a function of both frequency and depth reveals remarkable variability in the scattering cross section (Figs. 3–5). In each figure, contours of σ^T, σ^{sT}, and σ^{sTc} are compared. Only regions where $\sigma > 10^{-11}$ m^{-1} are contoured. This corresponds to scattering strengths $S_v \equiv 10 \log\sigma > -110$ dB, a cutoff somewhat below minimum measurable levels (Goodman 1990). Levels of σ vary by orders of magnitude in the vertical owing to variations in χ, ϵ, and δ.

Including salinity (σ^{sT}) extends the frequency range of measurable σ by roughly a factor of 10 above the temperature-only case (σ^T). For the shelf site (Fig. 3) the extension of measurable σ to higher frequencies occurs only over a limited depth range where χ and ϵ are large and δ is at a minimum. Elsewhere, including salinity makes no obvious change in the levels of σ

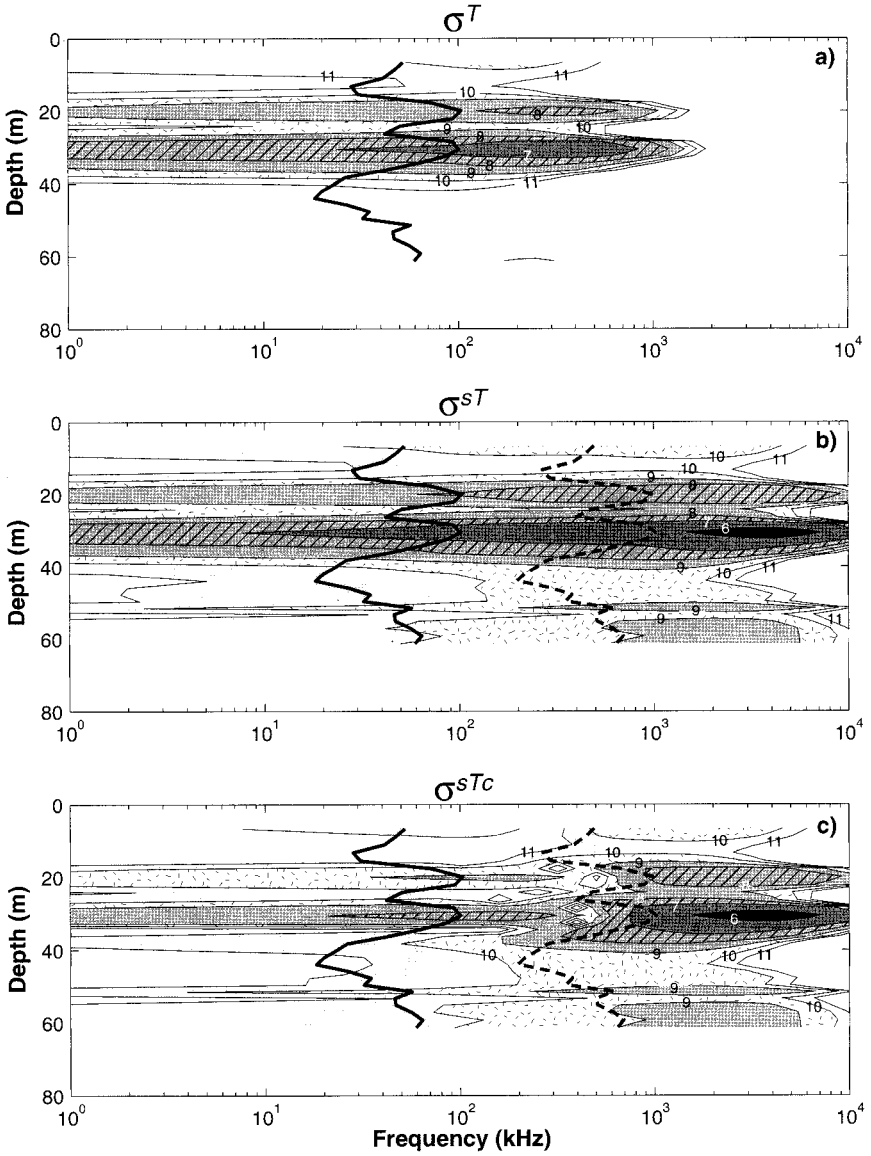

FIG. 4. Contours of σ as a function of depth and acoustic frequency for the Bosphorus. Panels are as in Fig. 3. Small δ causes the inclusion of salinity to dramatically alter σ. The cospectrum introduces deep, narrow notches near $f(k_d)$, where $R_\eta \approx -1.5$.

because $|\delta| \geq 5$. Predicted levels of σ are modest, the maximum values corresponding to a S_v of -90 to -80 dB in the main pycnocline on the New England shelf.

Including the cospectrum (σ^{sTc}) for the coastal site alters σ little. Levels of σ are slightly smaller and the only noticeable effect is a small dip in values between the peak response due to temperature and that due to salinity.

Quite the opposite is true for the Bosphorus and Puget Sound. Including salinity in the calculation of σ increases S_v by 1–10 dB at frequencies less than $f(k_{\text{int}})$. The increase is greatest below 40 m in the Bosphorus, where R_η falls below 0.5 (Fig. 1). Between $f(k_{\text{int}})$ and $f(k_d)$, σ increases by 2–20 dB at both sites. Above $f(k_d)$, the increase is tremendous. Maximum levels of σ occur at frequencies of 1 MHz and higher, a consequence of very large ϵ values. The maximum S_v for the Bosphorus is -57 dB, which is quite a large scattering strength.

The cospectrum has a much more noticeable effect at the estuarine sites than at the coastal site. Puget Sound is most strongly effected because $R_\eta \approx -1$ below 35 m. The strong returns below $f(k_d)$ predicted for σ^{sT} are negated by the cospectrum in the contours of σ^{sTc} (Fig. 5). For the Bosphorus, deep notches occur in σ^{sTc} between $f(k_{\text{int}})$ and $f(k_d)$ over 20–40 m, where $R_\eta \approx 1.5$.

The frequency range of maximum σ varies widely between sites. It is controlled by δ and ϵ. Although the shelf and Puget Sound have similar levels of ϵ, smaller

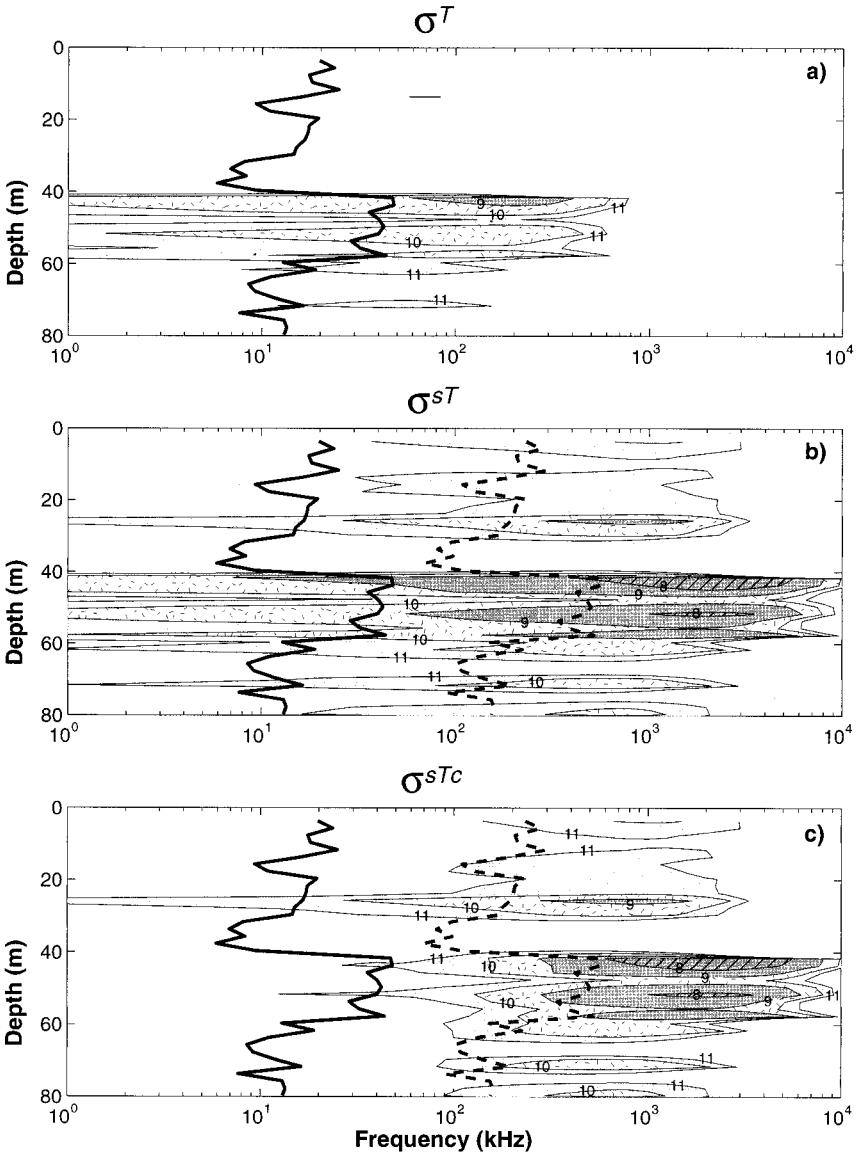

FIG. 5. Contours of σ as a function of depth and acoustic frequency for Admiralty Inlet in Puget Sound. Panels are as in Fig. 3. Including salinity greatly increases σ at all frequencies. The cospectrum strongly suppresses σ below $f(k_{\text{int}})$ because $R_\eta \approx -1$, leaving large σ only above 100 kHz.

δ in Puget Sound shifts maximum σ into the megahertz range, as compared to 100 kHz for the shelf. Despite comparable δ, the higher levels of ϵ in the Bosphorus, relative to Puget Sound, shift maximum σ to even higher frequencies, about 5 MHz. Since $k_d \propto \epsilon^{1/4}$, a 100-fold increase in ϵ leads to about a 3-fold increase in frequency of maximum σ.

5. Summary and discussion

Using observations from coastal and estuarine environments we predict that the magnitude and frequency dependence of the scattering cross section is strongly affected by salinity stratification. Our results assume a ''Batchelor'' spectrum of salt and that the dissipation rate of salinity variance is proportional to the square of the ratio of the mean salinity and temperature gradients times the dissipation rate of temperature variance. There have been no measurements of χ_s or a Batchelor spectrum of salt, but measurements of χ and the associated viscous–convective subrange of temperature abound and there is no reason to suspect our assumptions are ill-posed.

When $|R_\eta| \leq 1$ the salinity contribution to the scattering cross section is equal to or greater than the temperature contribution for $f < f(k_d)$. At higher frequen-

cies the salinity contribution dominates scattering and extends the frequency range by roughly a factor of 10 over that of a temperature-only spectrum. Neglecting the contribution of salinity in salt-stratified environments will lead to severe underestimation of the scattering strength at high frequencies.

The scattering cross section increases as f^{+1} between $f(k_{\text{int}})$ and $f(k_{ds})$ in this case. This is in contrast to the frequency dependence of σ^T: the viscous–convective subrange of temperature is too limited in bandwidth to display a true f^{+1} region. For very energetic turbulence, strong scattering can be expected to frequencies in excess of 10 MHz. The frequency dependence over a wide bandwidth may provide a method for distinguishing microstructure scattering from biological scattering.

In the very instances where salinity microstructure can enhance scattering, the cospectrum may act to reduce scattering. When δ is negative (either a diffusively stable or layering-favorable system) the cospectrum reduces the level of the refractive index spectrum: only for salt-fingering-favorable situations does the cospectrum increase the refractive index. The magnitude of the cospectrum depends sensitively on R_η; its maximum effect occurs for $R_\eta = 1$. When $R_\eta < 1$ the maximum effect occurs in the inertial convective subrange, while for $R_\eta > 1$ the maximum influence shifts to higher frequencies in the viscous–convective subrange for temperature. The results for large R_η suggest the notch narrows and deepens as R_η increases, but this is unlikely because it relies on a perfect correlation between salinity and temperature at the diffusive scales for temperature.

The cospectrum only effects frequencies less than those corresponding to k_d. Higher frequencies are unaffected, and we come to the curious result that salinity suppresses scattering at frequencies conventionally associated with temperature microstructure, and greatly enhances scattering at higher frequencies, up into the megahertz range.

The images produced by high-frequency systems have proven invaluable in understanding the processes generating intense turbulence in coastal waters. The high levels of S_v that microstructure can generate suggest that the images may in fact reveal the spatial distribution of scalar dissipation. If so, then acoustic backscatter measurements provide a unique and economical method to study spatial organization of turbulence. Confirmation of this intriguing possibility would certainly enhance the value of echosounding images to students of small-scale physical processes.

Multifrequency acoustic systems may be capable of distinguishing biology and microstructure in backscatter images based on spectral signatures. Validation of this ability will require accurate, simultaneous measurement of ϵ, χ, and σ, some confirmation of the viscous–convective subrange of salt, and zooplankton concentration measurements. The sampling requirements make this a daunting challenge, but the insight to be gained certainly will make the effort worthwhile.

Acknowledgments. This work was supported by the Office of Naval Research Grant N00014-96-1-0616. The author thanks Drs. Gregg (Bosphorus data) and Oakey (New England shelf data) for kindly sharing their observations.

REFERENCES

Armi, L., and D. M. Farmer, 1988: The flow of Mediterranean water through the Strait of Gibraltar. *Progress in Oceanography,* Vol. 21, Pergamon Press, 1–105.

Batchelor, G. K., 1959: Small-scale variation of convected quantities like temperature in turbulent fluid. *J. Fluid Mech.,* **5,** 113–133.

Bendat, J. S., and A. G. Piersol, 1986: *Random Data: Analysis and Measurement Procedures.* John Wiley and Sons, 407 pp.

Dillon, T., and D. Caldwell, 1980: The Batchelor spectrum and dissipation in the upper ocean. *J. Geophys. Res.,* **85,** 1910–1916.

Ewart, T. E., 1980: A numerical simulation of the effects of oceanic fin structure on acoustic transmission. *J. Acoust. Soc. Amer.,* **67,** 496–503.

Farmer, D. M., and J. D. Smith, 1980: Tidal interaction of stratified flow with a sill in Knight Inlet. *Deep-Sea Res.,* **27A,** 239–254.

——, and R. A. Denton, 1985: Hydraulic control of flow over the sill in Observatory Inlet. *J. Geophys. Res.,* **90,** 9051–9068.

Gargett, A. E., 1985: Evolution of scalar spectra with the decay of turbulence in a stratified fluid. *J. Fluid Mech.,* **159,** 379–407.

Goodman, L., 1990: Acoustic scattering from ocean microstructure. *J. Geophys. Res.,* **95,** 11 557–11 573.

Gregg, M., 1984: Entropy generation in the ocean by small-scale mixing. *J. Phys. Oceanogr.,* **14,** 688–711.

——, 1987: Diapycnal mixing in the thermocline: A review. *J. Geophys. Res.,* **92,** 5249–5286.

——, 1999: Uncertainties and limitations in measuring ϵ and χ_τ. *J. Atmos. Oceanic Technol.,* **16,** 1483–1490.

Haury, L., P. Wiebe, W. Orr, and M. Briscoe, 1983: Tidally generated high-frequency internal wave packets and their effects on plankton in Massachusetts Bay. *J. Mar. Res.,* **41,** 65–112.

Holliday, D. V., R. E. Pieper, and G. S. Kleppel, 1989: Determination of zooplankton size and distribution with multi-frequency acoustic technology. *J. Cons. Int. Explor. Mer.,* **41,** 226–238.

Macaulay, M. C., 1994: A generalized target strength model for euphausiids, with applications to other zooplankton. *J. Acoust. Soc. Amer.,* **95,** 2452–2466.

Oakey, N., 1982: Determination of the rate of dissipation of turbulent energy from simultaneous temperature and shear microstructure measurements. *J. Phys. Oceanogr.,* **12,** 256–271.

Seim, H. E., and M. C. Gregg, 1994: Detailed observations of a naturally-occurring shear instability. *J. Geophys. Res.,* **99,** 10 049–10 074.

——, ——, and R. T. Miyamoto, 1995: Acoustic backscatter from turbulent microstructure. *J. Atmos. Oceanic Technol.,* **12,** 367–380.

Stanton, T. K., P. H. Wieber, D. Chu, M. C. Benfield, L. Scanlon, L. Martin, and R. L. Eastwood, 1994: On acoustic estimates of zooplankton biomass. *ICES J. Mar. Sci.,* **51,** 505–512.

Thorpe, S. A., and J. M. Brubaker, 1983: Observation of sound reflection by temperature microstructure. *Limnol. Oceanogr.,* **28,** 601–613.

Washburn, L., T. F. Duda, and D. C. Jacobs, 1996: Interpreting conductivity microstructure: Estimating the temperature variance dissipation rate. *J. Atmos. Oceanic Technol.,* **13,** 1166–1188.

Wesson, J. C., and M. C. Gregg, 1994: Mixing at Camarinal Sill in the Strait of Gibraltar. *J. Geophys. Res.,* **99,** 9847–9878.

Wiebe, P. H., and C. H. Greene, 1994: The use of high frequency acoustics in the study of zooplankton spatial and temporal patterns. *Proc. NIPR Symp. Polar Biol.,* **7,** 133–157.